Invited Articles

Toward a fluid mechanics of suspensions

Jeffrey F. Morris*

Benjamin Levich Institute and Department of Chemical Engineering, CUNY City College of New York, New York, New York 10031, USA

(Received 12 August 2020; accepted 20 October 2020; published 24 November 2020)

Suspensions are considered from the perspective of development of their bulk fluid mechanics. Suspension mechanics has had a fluid mechanical basis since its inception, as description of the motion of such a mixture requires consideration of the coupling of fluid motions to the surface stresses driving motion on the particles. While it thus sits on a very firm foundation of prior study of the microhydrodynamics, i.e., the microscale forces and motions of the particles and their relation to the properties, the bulk fluid mechanics of suspensions is still in its early stages. This work first outlines the foundations and then proceeds to describe some basic developments from studies exploring the behavior of suspensions as bulk fluids. The focus is on the near-hard-sphere suspension of solid particles in Newtonian liquid, for which a coherent and extensive, though far from complete, understanding of properties and phenomena exists; an overview of the state of understanding of rheology and migration phenomena is provided. This is followed by a consideration of part of the rather limited body of work which explores a central fluid mechanical paradigm of the viscous-inertial balance, i.e., the influence of the bulk Reynolds number Re, emphasizing its impact on two flows studied by the author, namely stability of bulk suspensions in pipe and Taylor-Couette (TC) flows. In the TC flow, states not seen in pure fluids under similar conditions are observed. Similarly, elevated Reynolds number flow in bifurcating conduit flows is shown to challenge our ability to predict behavior based on continuum descriptions of the particle phase, indicating directions for productive study.

DOI: 10.1103/PhysRevFluids.5.110519

I. INTRODUCTION

Solid-liquid mixtures are found broadly and go by different names, e.g., slurries if they settle quickly and dispersions if the particles remain suspended. The flow of these mixtures plays an essential role across a rather large spectrum of societal concerns: Mudslides, blood flow, slurry extrusion, and concrete-based construction are longstanding issues where solid-liquid flows play a role, while inkjet printing and additive manufacturing techniques using dispersed solids are new applications that now challenge our understanding. Fluid mechanical understanding of dispersions of solids in liquids, in terms of both their basic properties and the impact of these properties on larger-scale phenomena, is clearly useful. For scientific study, a foundational model is needed, and for this purpose we consider suspensions, generally understood as materials in which the particles stay reasonably well dispersed.

In this article, which follows from the Stanley Corrsin Award lecture in 2019, an overview beginning from microhydrodynamics and microstructure of suspensions sets the stage for.a perspective

*morris@ccny.cuny.edu

on emerging topics in the fluid mechanics of suspensions. While a number of related studies are described, no attempt is made to provide a thorough review, and thus the focus is on work in which I have been involved and thus can speak with sufficient knowledge to build a relatively continuous narrative.

The discussion will focus on the simplest suspension that exhibits the prominent rheological features of suspensions, namely the near-hard-sphere suspension in Newtonian liquid. The material properties of suspensions remain a topic of intensive interest, but understanding of these properties is now quite advanced, whereas the "fluid mechanics of suspensions" remains a topic that is in its infancy—only a few of its features are becoming clear enough to define such a subject. To begin, in Sec. II I will define the conditions and the suspension model studied, to limit discussion to a manageable scope. Then I will consider the state of understanding of suspension properties, and with scope again in mind, it seems useful to present an outline of developments supporting a fluid mechanics of suspensions that have taken place over the last 50 years, conveniently dating from landmark work by Batchelor [1] that underpins much of the mechanical description. In Sec. III the rheological properties that make suspensions distinct from simple fluids, and the microhydrodynamic basis for understanding of these properties by means of simulation and theory is outlined. An important feature of suspensions is that the rheology leads to both secondary flows and to shear-induced migration, the latter a relative motion between the phases resulting in compositional variation; these have expected effects on the flow of the bulk mixture that can be observed in Stokes flow, and these are discussed in Sec. IV. Finally, work in which suspensions have been studied at finite Reynolds number is described, with Sec. V B considering stability of Taylor-Couette and pipe flows, while Sec. VI considers flow in the somewhat more complex case of branching conduits. To close, a perspective on the questions open to study is offered.

II. CONDITIONS AND THE MATERIAL MODEL

For basic understanding, only suspensions in Newtonian liquids will be discussed, and non-Newtonian behavior will thus arise from the particle interactions. Particles in more complex suspending fluids are considered elsewhere [2,3].

The conditions studied are defined in dimensionless terms. The particle Reynolds number $Re_p = \rho\dot{\gamma}a^2/\eta_0$ has its common meaning related to the balance of inertial and viscous effects, but at the scale of the particle radius a and for a shear flow with $\dot{\gamma}$ the shear rate. The Péclet number $Pe = 6\pi\eta_0\dot{\gamma}a^3/kT$ represents the ratio of shear to thermal motions. The density of both particles and fluid for a neutrally buoyant suspension is ρ, the suspending fluid viscosity is η_0, and the thermal energy is kT, where k is the Boltzmann constant and T is absolute temperature. The bulk Reynolds number is defined based on the flow scale, e.g., $Re = \rho UR/\eta(\phi)$ for pipe radius R, where $\eta(\phi)$ is the apparent viscosity as a function of the solid volume fraction ϕ, and is often stated in terms of the dimensionless relative viscosity $\eta_r(\phi) = \eta(\phi)/\eta_0$; often the two Reynolds numbers are related by the relationship $Re_p \sim (a/R)^2 Re$. For the most part, the study of rheology has focused on $Re_p = 0$; this will be specifically relaxed at the end of Sec. III. Finite Re_p effects resulting in particle migration are addressed in Sec. IV, and the influence of the resulting concentration variation will be considered in Secs. V B and VI. The strong variation of $Pe \sim a^3$ is important; as an example, increasing from $a = 1$ μm to $a = 10$ μm results in increase of $Pe = O(0.1)$ to $Pe = O(100)$ for particles in water at room temperature and $\dot{\gamma} = 1\ \mathrm{s}^{-1}$. One order of magnitude change in particle size thus moves us from a condition where Brownian motion is strong and readily observed to one where it is quite weak relative to even a modest shear rate. Only limited finite-Pe results are considered here in the discussion of rheology. A point worth noting is that it is quite difficult to have observable Brownian effects at the same time as significant particle-scale inertia, as the Schmidt number defined by $Sc = Pe/Re_p \sim \nu/D_0 \gg 1$, where $\nu = \eta_0/\rho$ is the kinematic viscosity and $D_0 = kT/6\pi\eta_0 a$ is the particle Brownian diffusivity: The molecular process of momentum diffusion is generally vastly larger than diffusion of particle mass, so that finite Re_p implies $Pe \gg 1$ such that thermal motion is largely negligible.

Faced with a solid-liquid mixture problem, there are different ways one might construct a model suspension depending on what mixture behaviors are of most interest. Here the goals are first to establish the suspension as a *material*, i.e., a mixture of well-defined constituents in definite proportions, whose properties can be measured and analyzed, and second to have a sufficiently simple model that theory, computational simulation, and experiment can converge. This convergence is beneficial as we seek to develop thorough understanding both of the properties and their influence in bulk fluid mechanical phenomena such as flow structures and stability. The model that has found the most use for describing basic physics of suspensions is the near-hard-sphere model, which is "as simple as possible, but not more so"—the NHS model retains the features necessary to capture the rheological phenomena in experimentally studied suspensions that are carefully designed to be close to hard sphere in nature.

The necessity in experimentally studied suspensions of some force in addition to the contact force that enforces excluded volume arises particularly for colloidal particles. Particles in liquids can interact through a number of different forces with interaction range varying widely depending on their composition and that of the suspending fluid, but one pervasive force is the van der Waals force arising due to differing polarizability between particles and liquid. This most often leads to attractions between particles whose surfaces are close, and can thus result in aggregation. To avoid aggregation, some slight surface charge to cause electric double layer repulsion or a short grafted molecular chain to induce steric repulsion may be used. Either of these forces can be tuned to be very short-ranged relative to the particle radius, an idea that is simply captured for theoretical calculations by the excluded annulus model [4]; here b is the radius of closest approach associated with the repulsive force, while a is the true hard sphere or hydrodynamic radius, and $b/a - 1 \ll 1$ for the NHS model. For larger particles, where the vdW force might be irrelevant, one still observes that the HS model is too restrictive, as it implies Stokes-flow reversibility of motions and this is not seen in reality. Here the idea of b/a slightly greater than unity may be considered to account for either finite-separation repulsions as described above or contact interactions that are important in compression, and thus lead to an asymmetry of the pair interaction. In simulations, a smooth but steep repulsive force for particles at small surface separation is often implemented [5], with this often thought of as a computational convenience.

However, because it breaks the reversibility of motion that is expected for hard spheres in Stokes flow [6], the repulsive force is more than simply a convenience. The consequences at pair level of the NHS model for Brownian suspensions pushed to the high-shear limit were developed by Brady and Morris [4], using the excluded annulus model: There it was found that as $Pe \to \infty$, the rheology is singular in the influence of the short range forces: Any finite $b/a - 1$ resulted in non-Newtonian behavior that was not present for the hard sphere case of $b = a$. For monodisperse hard spheres at $\phi > 0.5$ and only hydrodynamic Stoke-flow interactions at $Pe^{-1} = 0$, Ball and Melrose [7,8] showed that a suspension of solid volume fraction $\phi \approx 0.5$ computed with high accuracy will undergo what they termed "lubrication breakdown." Specifically, they found that the sheared suspension would reach unphysically thin—below molecular scale—liquid films between particle surfaces in less than a unit of strain. The computations being reversible, this means that the shear could in principle be reversed with all particles returning to their original position and then undergo this same sort of jamming event in the opposite direction of strain. This behavior is not observed in practice, as such concentrated suspensions lose reversibility over strain of $O(1)$ and typically can be made to flow at $\phi > 0.5$, although it is at about this solid fraction that hydrodynamic dominance of behavior breaks down; both points are discussed in Sec. III.

To complete the definition of the system studied here, we consider a suspension as a homogeneous material, and for this purpose we require that the particles be density matched to the suspending liquid. Density matching removes concern about segregation due to settling, with the result that the mixture can be considered as a relatively uniform bulk material whose properties can be conveniently measured. To simplify as much as possible, we limit consideration to relatively monodisperse suspensions, but allow particle size to be an essential variable in the model.

It is worth considering briefly what is discarded in the NHS model. Long-range electric double layer repulsion, due to particle surface charge interaction with soluble ions, and direct Coulombic forces that are found, for example, in the clays within mud are not captured, and these can lead to yield stresses. Considering only relatively rigid particles eliminates the influence of pronounced deformation, and thus the behavior of blood, with its relative ease of flow as the red blood cells deform to slip past one another under normal conditions, is not well represented; this suggests the importance for ease of flow of the deformability, and the detrimental biological consequences of the tendency to jam of rigidified and sickle shaped cells in the devastating pathology of sickle cell disease [9]. Finally, the restriction to spherical particles must be relaxed to consider fiber-laden fluids as found in papermaking, or the detailed motions in shear flow of platelike particles as in the case of the noted clays or blood platelets. Thus what is said in the following applies directly to the more basic suspensions, but may serve as foundation and guidance toward work on these microscopically complex materials.

III. RHEOLOGY

The rheology of near-hard sphere suspensions is not only influenced by (in fact, at dilute to moderately concentrated conditions, largely controlled by) fluid mechanics, but also impacts on the observed large-scale fluid mechanical behavior.

A. Microhydrodynamics

Fluid mechanics enters at the particle scale in suspensions, as one important task is to understand how microscale flow (or microhydrodynamics as it was named by Batchelor [10]) results in the suspension stresses and then translate this to appropriate average results useful at the macroscopic scale. Suspension rheology relies on fluid mechanics at this scale to describe the influence of hydrodynamic interactions between particles. Einstein's 1906 publication [11] was the first to show how a single particle immersed in a straining flow leads to an added dissipation rate because of the flow disturbance it creates, with the apparent viscosity $\eta_E = \eta_0(1 + 5\phi/2)$. A number of further results for single particles were developed and these are well summarized by the book by Happel and Brenner [12] originally appearing in 1965, and first effects of particle interactions have been considered for sedimentation velocity and viscosity by methods introduced by Batchelor [13–15]. Although important, this direction of work is limited in validity to $\phi \ll 1$, and we leave most of it aside to focus on bulk suspension behavior at larger ϕ.

Toward larger-ϕ work, the 1970 work of Batchelor [1] using an ensemble average approach to define the bulk suspension stress has been influential. From this work, a crucial result is that for a homogeneous system, the ensemble average hydrodynamically determined stress for N particles in a volume V may be written in terms of volume averages as

$$\Sigma_{ij} = \frac{1}{V}\int_{V-\sum V_0}[-p\delta_{ij} + 2\eta_0 e_{ij}]dV + \frac{1}{V}\int_{\sum V_0}\sigma_{ij}dV - \int_V \rho u_i' u_j', \tag{3.1}$$

where $\sum V_0$ is the sum over all particle volumes, σ_{ij} and $e_{ij} = (\partial u_i/\partial x_j + \partial u_j/\partial x_i)/2$ give the components of the stress and rate of strain, respectively, and $\mathbf{u}'$ represents a velocity fluctuation. Using the divergence theorem to express the stress within the particles as

$$\int_{\sum V_0}\sigma_{ij}dV = \int_{\sum S_0} x_j\sigma_{ik}n_k dV - \int_{\sum V_0}\frac{\partial\sigma_{ik}}{\partial x_k}x_j dV dS,$$

denoting all particle surfaces by $\sum S_0$, yielded the form for rigid particles of

$$\Sigma_{ij} = -\frac{\delta_{ij}}{V}\int_{V-\sum V_0} pdV + 2\eta_0 E_{ij} + \Sigma_{ij}^P, \tag{3.2}$$

$$\Sigma_{ij}^P = \frac{1}{V}\int_{\sum S_0} x_j\sigma_{ik}n_k dS - \frac{1}{V}\int_{\sum V_0} F_i' x_j dV - \frac{1}{V}\int_V \rho u_i' u_j' dV, \tag{3.3}$$

where E_{ij} is the bulk average rate of strain. The term with F_i' arises by writing $\partial\sigma_{ij}/\partial x_j = F_i'$ inside the particles, while the final term is equivalent to a Reynolds stress in turbulent flows. In the original derivation, the $F_i'x_j$ term is thus associated with fluctuating accelerations of the particles and is little studied in that context; this term is often used as motivation for the stresses arising from conservative interparticle forces (xF stresses) of the same form.

The first term on the right-hand side of (3.3) is a moment of the surface traction giving in symmetrized form the hydrodynamic stresslet for a single particle $S_{ij} = (1/2)\int_{S_0}(x_j\sigma_{ik} + x_i x_i\sigma_{jk})n_k dS$, which is the contribution resulting in the Einstein correction in the dilute limit. In this limit, $S_{ij} = (20\pi/3)\eta_0 a^3 E_{ij}$ for a sphere of radius a, and when multiplied by the number density $N/V = 3\phi/(4\pi a^3)$, this yields a contribution to the bulk stress of $5\phi\eta_0 E_{ij}$, and recalling that the shear stress is $2\eta E_{ij}$, this yields the ϕ-dependent term in the (Einstein) effective viscosity of $\eta_E(\phi) = \eta_0(1 + 5\phi/2)$. The stresslet term can be evaluated for concentrated suspensions if the relative motions of particles are known.

Application of these results was facilitated by the systematic development of hydrodynamic interaction theory for pairs of particles, in particular by Jeffrey and co-workers [16,17]. These interaction functions, describing for example the hydrodynamic force on a particle due to velocity in the form $\mathbf{F}^H = -\mathbf{R}_{FU}(\mathbf{x}^N)\cdot\mathbf{U}$, where the resistance function $\mathbf{R}_{FU}$ is shown to be dependent upon the full N-body configuration $\mathbf{x}^N$, were used to develop the Stokesian dynamics simulation method [5]; similar forms are available for the torque and stresslet, and for all to couple to velocity, rotation, and strain rate. The SD approach provides a molecular-dynamics-like approach to discrete-particle simulation. The method relies on an approximation for the many-body interactions developed based on the paradigm of splitting to close or near-field interactions (based on lubrication descriptions) and far-field descriptions based on response to force multipoles; more recent methods have improved the speed of this method to allow computation of larger numbers of spherical particles in acceptable time [18,19]. With the combination of discrete-particle simulation and a mechanistic framework for describing the stress contributions due to different mechanisms, the stage was set for exploration of the microscale mechanics and their coupling to bulk flow properties. Other simulation tools have been developed that allow for inclusion of fluid inertia and results of these are discussed below, but SD retains a special role in development of understanding of the microstructure and rheology of suspensions.

B. Properties

As the particle solid fraction ϕ varies from dilute to highly concentrated or "dense," suspensions of near-hard spheres exhibit properties that vary from those of the suspending fluid with small quantitative variations to a complex fluid whose properties may be difficult to measure, and whose behavior is frequently difficult to predict in applications. The rheological properties, exemplified by effective viscosity $\eta(\phi)$, vary strongly with ϕ, with a typical form expressing the relative viscosity as

$$\eta_r(\phi) = \frac{\eta(\phi)}{\eta_0} = \left(1 - \frac{\phi}{\phi_J}\right)^{-\alpha}, \quad \alpha \approx 2, \tag{3.4}$$

where η_0 is the suspending fluid viscosity; ϕ_J is the jamming fraction, and this name, rather than maximum packing fraction ϕ_{max} often used in previous suspension work, reflects recent directions of study. These emphasize the importance of the closeness to jamming conditions, where imposing shear stress causes formation of a jammed solid and it is explicitly recognized that ϕ_J depends on the stress level [20]. More generally, rate dependence is critical in the rheological properties. Well below the jamming fraction, suspensions exhibit rate dependence in their viscosity, on which there is a large literature to which the text by Mewis and Wagner provides guidance [21]. One point worth noting is that simulations by the Stokesian dynamics method [22,23], incorporating just Stokes flow and Brownian motion, are able to capture the shear-rate dependence measured experimentally [24,25] in carefully made near-hard-sphere suspensions for $0.3 < \phi < 0.5$ over about six decades

of shear rate, $10^{-3} \leqslant Pe \leqslant 10^3$, but the higher volume fraction data where shear thickening is very pronounced [25] is not captured by my own simulations using the same technique [26], which motivated work to incorporate contact interactions, as briefly described in Sec. III D.

Suspensions also exhibit a normal stress response, and while the magnitude of the stress is roughly linear in the shear rate, this is intrinsically a nonlinear response, as the geometric form of the flow-induced stress tensor does not mirror that of the rate of strain. The normal stress differences, given in terms of the flow (1), gradient (2), and vorticity (3) directions of a viscometric flow as $N_1 = \Sigma_{11}^P - \Sigma_{22}^P$ and $N_2 = \Sigma_{22}^P - \Sigma_{33}^P$ (superscript P to indicate that the normal stresses arise from the particle stress) are commonly encountered in rheology of viscoelastic fluids. However, in suspensions all of the Σ_{ii}^P terms are compressive for the materials considered here. Measurements of normal stress differences have been made for noncolloidal [27,28] and colloidal suspensions [29], and generally find N_2 negative; $N_1 < 0$ is typically found until ϕ is sufficiently large that strong shear thickening occurs, at which point a so-called dilatant response $N_1 > 0$ may be found [30]. The normal stresses have well-known effects on free surfaces—causing a rod climbing in viscoelastic materials and rod dipping [27,31] in suspensions—and on streamlines [32] as considered in Sec. V.

While it is not a subject of classical rheology, the mean normal stress of the particle phase, written in the negative form $\Pi = -(1/3)[\Sigma_{11}^P + \Sigma_{22}^P + \Sigma_{33}]$ reflects the tendency to spread of a clump of suspended particles by a flux $\mathbf{j} \sim -\nabla\Pi$; it is given by the equilibrium osmotic pressure $\Pi/nkT = 1 + 4\phi g_{\text{cont}}$ for hard spheres in the absence of flow, where g_{cont} is the contact value of the pair distribution function and reflects the influence of excluded volume. When shear flow is imposed at high Pe, this shear-induced osmotic pressure scales as $\Pi \sim \eta_0 \dot{\gamma} \eta_n(\phi)$, where $\eta_n(\phi)$ is the so-called normal stress viscosity [33] and diverges in the same way as $\eta(\phi)$ for $\phi \to \phi_J$.

Thus, not only does $\nabla\phi$ drive a flux (Fickian diffusion), but a macroscopic $\nabla\Pi$ will arise in flows with spatially varying shear rate, driving a shear-induced migration flux, i.e., $\mathbf{j}$ as above, which causes nonuniform particle concentration; this makes the particle pressure a quantity of relevance to determining the phase distribution and thus the mixture properties as addressed in Sec. IV. Note that Batchelor [1] described the isotropic stress as "of no intrinsic interest," apparently based on the absolute pressure being irrelevant due to incompressibility. However, the particle and fluid phases in a suspension are compressible—they can change their local concentration. Thus, an elevated particle stress tending to disperse the particle phase implies that the liquid phase must be in tension relative to the surroundings: This agrees with an osmotic conception of the normal stresses and has been used to measure the shear-induced suspension normal stress [34,35]. Alternative methods based on equilibration of the liquid pressure across a screen [36] date to a pioneering work by Prasad and Kytomaa [37].

As a final point, we note that the influence of inertia at microhydrodynamic scale, and thus a dependence of the rheology on the particle Reynolds number Re_p has been considered since the 1970 work of Lin, Peery, and Schowalter [38], appearing in the same year as Batchelor's paper on the suspension stress system [1]. However, this topic has advanced much less than Stokes-flow rheology. The influence of microscale inertia has been explored primarily through numerical simulation at single-particle, pair, and many-body level, with related work on suspended drops also known [39]. The observed behavior includes loss of fore-aft streamline symmetry about the particle, allowing non-Newtonian response at single-sphere level [40,41], surprising spiralling interactions of isolated pairs [42] whose residual effects are found even at rather significant concentration [43], and inertial thickening [40]. Experiments show that inertia will tend to make particles migrate due to interaction with walls and spatial gradients in shear rate, as outlined in Sec. IV. A more difficult, and perhaps the most challenging, point is that microscale inertia implies quite large macroscopic inertia: For particles in a pipe flow with radius ratio $R/a = 50$, $Re_p = 1$ would imply $Re = (50^2)Re_p = 2500$ and thus instability is expected. Larger-scale inertial effects in suspensions are considered in Sec. V.

C. Microstructure

While the viscosity of suspensions is readily appreciated just from nondeformability, explanation of its extreme variations with rate require a microscopic understanding of flow-induced correlations.

The more qualitative rheological differences of suspensions from the suspending fluid, e.g., the normal stress response, require development of microstructural anisotropy, in particular breaking the so-called fore-aft symmetry [4,44] of shear flows. The most basic model, hard spheres at $Re = 0$ and $Pe = 0$, leads to the expectation that the flow is reversible and thus will have fore-aft symmetry. This motivates understanding the role of Brownian motion and interparticle forces on the structure, which here is described primarily in terms of the pair distribution function $g(\mathbf{r})$, the likelihood of finding a pair of particles with center separation $\mathbf{r}$, relative to the mean pair density.

Early work from the period under consideration sought to determine how flow induced organization of the particles, or microstructure. The analytical study by Batchelor and Green [13,14] showed that Stokes shear flow of hard spheres in the absence of Brownian motion tends to cause accumulation at pairs at contact, but the predicted structural distortion from equilibrium was isotropic under these conditions. The Smoluchowski equation approach for particles subject to Brownian motion in a weak shear flow was later shown by Batchelor [45] to result in an $O(Pe)$ quadrupolar distortion of the pair distribution, i.e., $g(\mathbf{r}) = g_{\text{eq}}(r)[1 + Pef(r)\mathbf{r} \cdot \mathbf{E} \cdot \mathbf{r}/r^2 + \cdots]$ with $f(r) \sim r^{-3}$, but this level of description was insufficient to determine non-Newtonian effects. Brady and Vicic [44] carried the dilute microstructural analysis to higher order in Pe to describe the flow-induced structure necessary for normal stress differences (NSD). Brady and Morris in 1997 presented calculations of $g(\mathbf{r})$ at $Pe \gg 1$ under these small-ϕ conditions [4], showing the noted singularity to short-range forces of the structural asymmetry giving rise to the normal stress response. The microstructure in pure extension of dilute rough spheres has been considered using a similar approach by Wilson [46].

The observation from experiment [47] and simulation [22,26] is that shear induces a pronounced fore-aft asymmetry, with an extreme build-up of particle pairs near contact in the compressional quadrant of shear flow and depletion in the extensional quadrant. This asymmetry gives rise to the NSD [4] and also to the particle pressure [48,49]. The emphasis here on steady shear flow is sufficient to describe the normal stress and shear stress response crucial to understanding why and how suspensions differ from single phase flows. The coupling of structure to rheology is developed in earlier reviews [50,51]. Since the appearance of these reviews, theory has been advanced that extends Smoluchowski equation analysis to predict the high-ϕ structure and rheology [52], with alternative but related approaches based on density functional theory also now available [53].

The constitutive modeling even for smoothly shearing suspension flows remains a topic of significant interest and poses particular challenges in the $Pe \to \infty$ limit [54–56]. Nonetheless, the overall picture is that the structure becomes highly anisotropic, resulting in normal stress differences and particle pressure, and with extremely high probability of the so-called contact interaction. The likelihood of close interactions combined with the lubrication breakdown phenomenon noted in the prior section [7,8] led to a consideration in recent years of contact interactions and the development of force chains through the materials, particularly in highly concentrated, or dense suspensions. This relates to shear thickening and jamming, a topic treated in the following section.

D. Recent work: Discontinuous shear thickening

In the last decade, a surge of interest has been seen in the behavior of dense suspensions, at concentrations approaching the jamming fraction. This work has been focused around the phenomenon of strong shear thickening, which in its extreme case at sufficiently large ϕ can appear as a discontinuous rise in shear stress or viscosity (and normal stress) at a particular shear rate. This topic is addressed in detail in a separate review [20], where the relationship of dense suspension thickening due to a stress-induced contact network to jamming is emphasized. The basic idea that has been advanced [57–59] is that short-range repulsive surface forces maintain a separation between particles at small applied stress, and when this stress level is surpassed, the lubrication film is broken such that either contact friction [57,59] or an altered hydrodynamic interaction due to asperities [60] is activated. This exchange of dominant mechanism is able to capture much of the observed behavior, but it is clear now that it is oversimplified and the detailed mechanics of the

contact interactions of small particles must be better understood to advance this topic further. Thus, surface science and tribology interact with the microscale flows in the rheology and larger-scale fluid mechanics of this system. A number of papers addressing the overall behavior of dense suspensions with considerations across the various length scales can be found in a recent special issue of J. Rheol. [61].

At the larger scales where one can speak of the bulk fluid mechanics, shear-thickening systems have been shown to exhibit a vorticity-directed motion of a shear band [62] consistent with theoretical predictions based on fluctuations in the particle pressure [63] coupling to particle flux. Similar ideas were advanced to explain oscillatory rheology of very dense suspensions [64]. This two-phase coupling is a hallmark of suspension flows, and these studies show that it may cause instabilities even when inertia is absent.

IV. MIGRATION AND MULTIPHASE EFFECTS

Given the rheological properties of suspensions for uniform conditions, one can insert the results into the stress constitutive description and use this in the momentum equation for flow analysis. However, owing to the finite size of the particles, migration relative to the suspending liquid is observed. This phenomenon is not unique to suspended particles, as it is seen in polymeric systems [65], but it is stronger and more influential here because the particle size is larger than soluble polymer and often not so well separated from the bulk flow scale.

We emphasize that there are two quite distinct types of particle migration in NHS suspensions in Newtonian liquids. One migration is due to inertial effects, and is describable at single-sphere level. The other is rheologically driven: Typically called shear-induced migration, a bulk suspension behavior that requires that ϕ be sufficiently large for significant particle interactions, although it has been reported in Brownian suspensions at $\phi < 0.05$ [66]. As predictions of these separate mechanisms do not follow the same lines of reasoning, they are discussed separately. A study where the two mechanisms are shown to influence the distribution of particles is that of Han *et al.* [67].

A. Inertial migration

Observations of inertial migration date to circular tube flow studies of the phenomenon by Segré and Silberberg [68] in the early 1960s. This work found that the migration of neutrally buoyant particles at low channel Re is to a ring at $r/R \doteq 0.6$, where R is the tube radius, with progressive increase of the radius of this Segré-Silberberg (SS) annulus with increase of Re. The force driving the motion has been analyzed, by methods originating with concepts developed by Saffman [69], for pressure-driven channel [70–72] or tube flow [73]. Our [74] experimental study characterized this increased radial location at an axial distance from entry of $L/D \doteq 310$, showing that the accumulation on the SS annulus, where the lateral force vanishes, continues even into the intermittent turbulent regime, the onset of which is influenced by the particles (see Sec. V B). This work found what appeared to be accumulation on both the SS annulus and a smaller radius annulus for $Re > 400$, leading to the noted theory for the tube flow [73], which still found only a single near-wall equilibrium point at these elevated Re. This "inner annulus" was also observed by Morita *et al.* [75], but these authors showed that this is a transient feature that eventually vanishes at larger L/D, with the necessary $L/D > 1000$ for $Re > 800$. Morita *et al.* discuss the possible importance of the lateral driving force in the entry region of the flow where the flow is developing to explaining this behavior; particle motion in such an axially developing boundary layer is certainly a point of interest.

We now consider migration in the Couette geometry. Halow and Wills [76] observed inertial migration in the circular Couette flow regime, finding the particles to migrate to near the center of the Couette gap. The migration in Taylor-Couette flows has been considered in my own work [77], some reproduced in Fig. 1. For these experiments at low average solid fraction $\phi = 0.001$, and inner to outer radius ratio $r_i/r_o \doteq 0.88$, the migration is to a position of roughly 0.4 of the annulus width

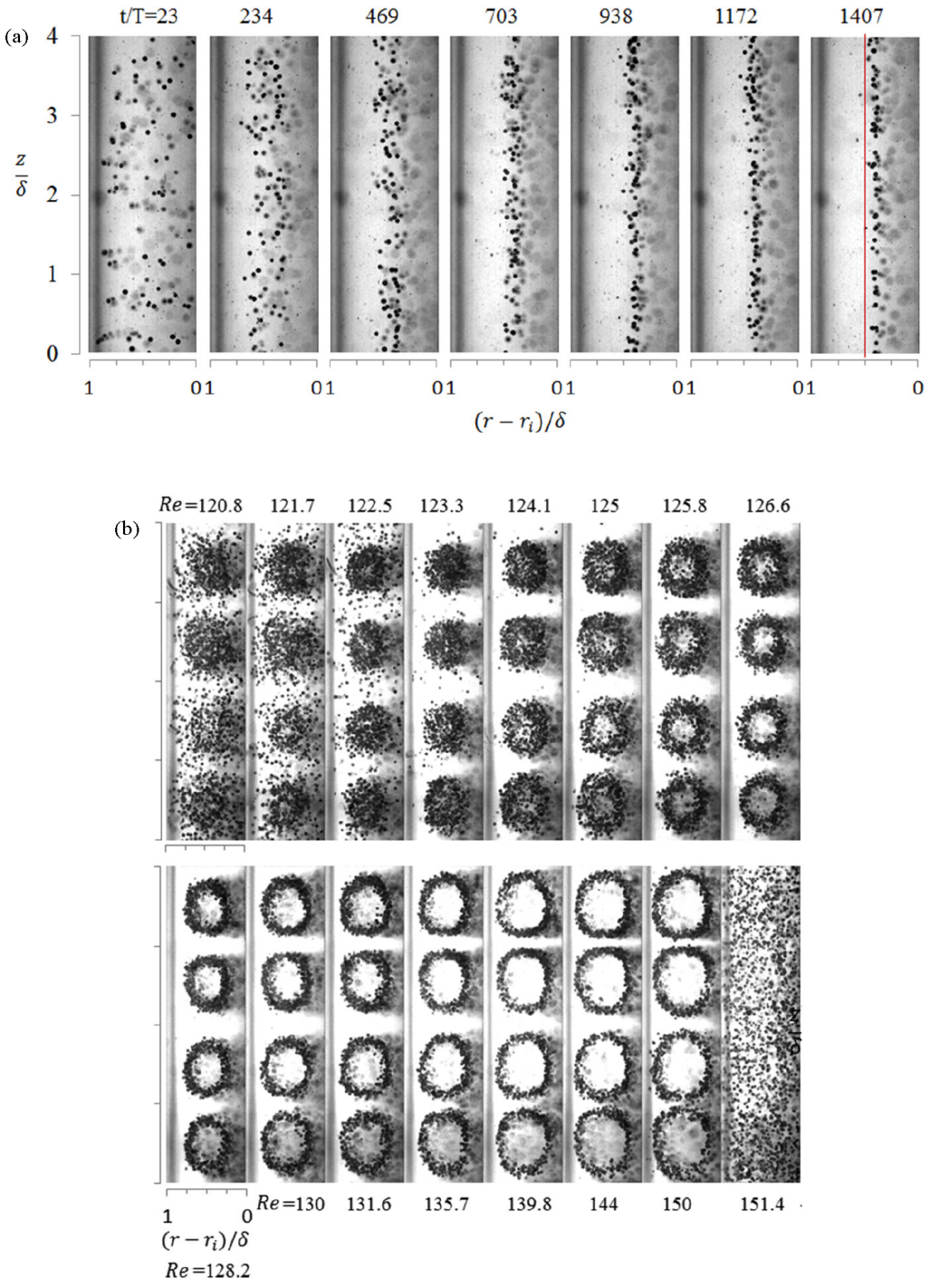

FIG. 1. Migration of neutrally buoyant particles in Taylor-Couette flow, adapted from work of Majji [77]. (a) Migration in circular Couette flow, with time shown in units of T, the period for one cylinder rotation. (b) Steady results following migration in the Taylor vortex flow, showing the variation in the particle distribution with Re based on inner cylinder rotation with the outer fixed. Here $\phi = 0.001$ and the ratio of inner to outer cylinder radii is $r_i/r_o \doteq 0.88$.

$\delta = r_i - r_o$ from the inner cylinder. When $Re = \rho\Omega r_i\delta/\eta_0$ where Ω is the rotation rate is increased beyond the transition to the Taylor vortex flow at $Re = 120$, the driving force associated with the dominant angular flow (the same as in the Couette flow regime) is coupled with the convection by the secondary vortex flow to result in particle accumulation that reflects the underlying flow. For $Re < 125$, the particles are progressively focused toward the center of each vortex, and further increase of Re results in development of a limit cycle of circular form within each vortex. With increase of Re, the diameter of this circle increases and the distribution sharpens until the onset of wavy Taylor vortices at $Re = 151.4$, in which flow the particles do not display nonuniformity of distribution. The inertial migration results in a history dependence of flow properties, and the implications for the bulk flow behavior of much more concentrated suspensions in TC flow are considered in Sec. V B.

Microfluidic devices often make use of inertial migration, e.g., toward separation [78], and in the typical square or rectangular cross section of these devices, the migration leads to accumulation of particles at a number of points in the cross section rather than an annular ring found in circular tubes. This was first shown numerically by direct calculations [79], and can be determined by iteratively seeking the points within the cross section of zero lateral force, based on steady calculations [80]. At sufficient ϕ that interactions take place, the migration combined with boundary effects can lead to preferred spacings [81] that in tube flow form many-particle "trains" [82], an observation also made in the early work of Segré and Silberberg [83]. By combining inertial migration with Dean flow in curved microchannels [84], the rate of migration can be enhanced, a point of some interest for application in separation of cells or assaying beads in biomedical applications [85].

B. Shear-induced migration

Shear-induced migration (SIM) refers to the low-Reynolds-number redistribution of particles, typically at moderately to highly concentrated ϕ, in shear flows. The first conclusive observation of SIM was made by Leighton and Acrivos [86] in the context of a rheometric experiment. Earlier evidence for nonuniform distribution of particles in pressure-driven flow at more elevated concentrations was found in blunted velocity profiles [87], but the first clear experimental evidence of SIM in pressure-driven flow was given by Koh *et al.* [88], with simulation of this flow in monolayer geometries by Nott and Brady [89]. As this topic has been reviewed in detail elsewhere [50,51], we touch only on the underlying dependence on microstructural distortion of SIM and how this process relates to bulk flow.

Modeling of SIM based on what has become known as the "diffusive flux model" was proposed based on the observations of Leighton and Acrivos by Phillips *et al.* [90]. This approach argues that particle flux is toward lower shear rate, a result in conflict with certain observations in torsional flows [33], prompting theory relating the migration to the normal stress response [33,89]. In brief, this "suspension balance model" (SBM) is based on coupling of the conservation of mass and momentum for the particle phase. The particle phase momentum is governed by

$$0 = \nabla \cdot \mathbf{\Sigma}^P + n\mathbf{F}^H, \tag{4.1}$$

where a linear law $\mathbf{F}^H = -6\pi\eta_0 a\mathbf{R}(\phi)(\mathbf{u}_P - \mathbf{u}_{\text{susp}})$ relates the drag to the difference between the mean particle and suspension velocities $\mathbf{u}_P - \mathbf{u}_{\text{susp}}$, with $\mathbf{R}$ a resistance tensor that can be estimated by the sedimentation hindrance function $f(\phi)$ [91,92]. This indicates that a migration is driven by the particle stress divergence $\mathbf{u}_P - \mathbf{u}_{\text{susp}} \propto (a^2/\eta_0 f)\nabla \cdot \mathbf{\Sigma}^P$. To complete a description of the flow, one must solve for the bulk suspension motion governed by

$$\nabla \cdot \mathbf{\Sigma} = 0 \quad \text{and} \quad \nabla \cdot \mathbf{u}_{\text{susp}} = 0, \tag{4.2}$$

with proper accounting of the spatial variation of the viscosity, and use the particle velocity in the conservation equation for particle mass. The normal stresses are responsible for the motion across the streamlines, and thus the bulk motion with evolving concentration gradient can be related back to the microstructural distortion.

While there is some debate regarding the proper closure, the rheological basis for migration in the spatial variation of normal stresses proves broadly applicable. The general approach of Morris and Boulay [33] described above also provides good predictions of the migration behavior of NHS colloidal suspensions when Brownian stress is included in $\mathbf{\Sigma}^P$ [93], and the pattern formation of electrorheological suspensions can be described with the method through inclusion of electrical stress [94]. Efforts to develop the approach for general kinematics have also been made [95], but there remains much to be done in this direction of study.

V. SECONDARY FLOWS AND INSTABILITIES

Development of the bulk rheological properties in steady-state suspension flow, and phenomena that have two-phase character—in the sense of a change in the concentration of the particles—have been outlined in prior sections. This provides the foundation for considering examples of bulk suspension flow behavior that can be ascribed to rheology or migration-induced concentration variation; work which considers such phenomena without inertial effects is considered first.

A. Rheological flow alteration and secondary flow

Because the migration phenomenon discussed in Sec. IV leads to a spatially varying concentration field, it will alter the observed flow in most circumstances. When the kinematics is controlled, as in rheometric parallel-plate or cone-and-plate torsional flows, this will not be the case and migrations in these flows [33,96] will affect the stress and thus complicate measurements of properties. However, in flows where migration can occur in the direction of the velocity gradient (the 2 direction of a viscometric flow as described in the prior section), significant alteration of the velocity profile can be developed. This is most readily appreciated for Poiseuille flow, which becomes "blunted" relative to the quadratic profile as particles accumulate near the centerline [88,89]. Alteration of the velocity profile in wide-gap Couette flow is also significant [33,90].

The blunting is a straightforward and readily captured phenomenon. A less obvious result is secondary flow caused by normal stresses. Giesekus [97] showed that in a noncircular conduit the presence of a second normal stress difference gives rise to a secondary flow, predicted to form closed orbits when projected to the cross section and spirals as the flow progresses axially [98], a behavior experimentally confirmed for suspension flow by Zrehen and Ramachandran [32]. This phenomenon is notable in its lack of a dependence on particle size, whereas the cross-stream motion by migration is proportional to a^β with $\beta = 2$ in the basic theory [33]. The implications for distribution of particles in the cross section are significant.

The phenomena described in this section can be observed under Stokes flow conditions, whereas those described immediately below are inertial in origin.

B. Inertial instability

Inertial instabilities are one of the true hallmarks of fluid mechanics, and thus there is a vast body of work devoted to this topic for single-phase fluids. The onset of turbulence in pipe flow and the sequence of instabilities observed in the Taylor-Couette flow between concentric cylinders, with one or both rotating, are among the best known. These two flows have been examined for instability of suspensions, and thus will be discussed here. We avoid consideration of instability phenomena in segregated systems, for example when particles settle into a layer that may undergo surface rippling, taking the view that this is as an instability in the fluid-structure interaction rather than an instability of a fluid material.

1. Taylor-Couette flow of suspensions

The influence of suspended particles on the Taylor-Couette (TC) flow has recently been addressed for moderately concentrated suspensions in my own work and several other studies. While it has

some applications that have motivated suspension flow work [99], it is its known rich behavior for single phase flow [100], combined with the relative convenience of its experimental setup in a small footprint device, that make the TC flow a clear candidate for exploration of stability of suspension flows. As we will see, the behavior is even richer than in single-phase flow, as the role of time—i.e., the history of the flow—becomes a factor. This complication arises because one must consider the migration phenomena described above as part of the picture.

Early work in this topic by Ali *et al.* [101] analyzed the linear stability of Couette flow for dilute suspensions, predicting that the particles would lead to lower-Re instability than seen for the pure fluid. While their own experiments did not show this behavior, experiments by Majji *et al.* [102] showed that the loss of stability of circular Couette flow (CCF) for a neutrally buoyant suspension occurred at progressively lower $Re(\phi) = \rho\Omega r_i \delta/\eta(\phi)$ as ϕ was increased. This work considered only a rotating inner cylinder with outer cylinder fixed, and in $Re(\phi)$ defined here, we specifically mention ϕ in the argument of Re to indicate the use of $\eta(\phi)$, the effective suspension viscosity accounting for the increased dissipation due to the particles. The particle sizes studied yielded $\delta/a \approx 30$ and 100, with the same general findings for both sizes, but with the influence of particles less pronounced as the particles became smaller (i.e., as δ/a increased). The onset of instability in the TC device with $r_i/r_0 = 0.88$ was found to decrease roughly linearly with ϕ from $Re = 120$ to 75 with change in solid fraction from $\phi = 0$ to $\phi = 0.30$. For $\phi \leqslant 0.05$, the instability gave rise directly to Taylor vortex flow (TVF), as expected for a pure fluid, but for larger ϕ, the initial instability was always to nonaxisymmetric states (spiral vortex flows, SVF, and superposed opposing spirals known as the ribbon structure, RIB) in the range $0.05 \leqslant \phi \leqslant 0.20$, before the TVF was reached at higher Re. At $\phi = 0.3$, the TVF was not reached as the sequence was CCF to SVF at $Re = 75$, to a wavy vortex flow that persisted in the range $82 < Re < 145$; as the range of Re at which TVF was seen decreased with ϕ, to the range of roughly $102 < Re < 107$ at $\phi = 0.20$, there is reason to believe the TVF state is not to be found for $\phi = 0.30$.

The main observations regarding new flow states from Majji *et al.* up to their limiting $Re \approx 165$ have been verified by Ramesh *et al.* [103], whose study went to slightly higher Re for $\phi \leqslant 0.25$. This work emphasized the hysteretic nature of the flow transitions. These effects are seen in slow up- or down-ramp protocols for varying Re used in both studies [102,103]. Figure 2 is reproduced from Ramesh *et al.* to illustrate the pronounced hysteresis: As an example, the SVF state seen in a slow down ramp of Re is absent in an up ramp. It is important to note that these ramps are

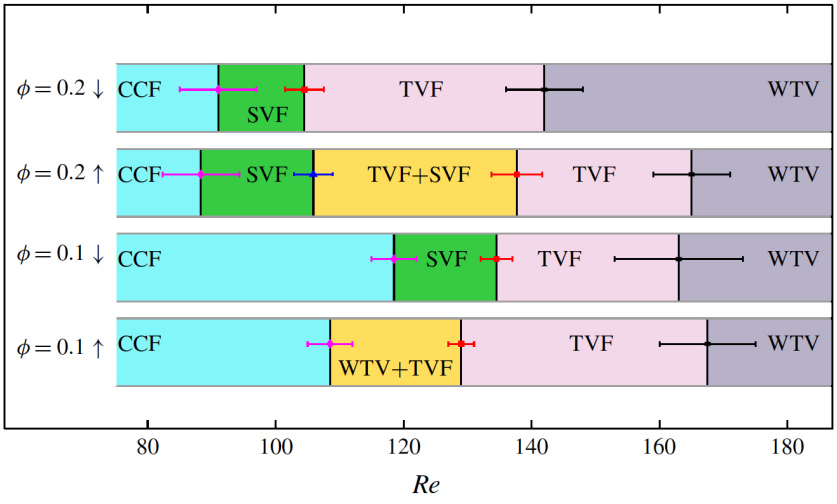

FIG. 2. Flow state diagram in Taylor-Couette flow of suspension. Differing position of state boundaries and different sequences of states for up and down ramps of Re show hysteresis. From Ramesh *et al.* [103].

purposely made sufficiently slow that rate effects known to affect transitions in pure fluids are not present. What is likely a more important factor is that the slow ramping allows inertial migration of the particles to cause significant nonuniformity in concentration, as illustrated for very dilute ϕ in Fig. 1. Importantly, Ramesh *et al.* also performed velocimetry that beautifully illustrates the intricate flows, while it also raises many questions. One is related to the observation of unexpected variation in the shear rate within the CCF regime, and one may wonder if the particle migration is the source. Our own recent work in which the migration effects at $\phi = 0.10$ are specifically studied by protocols that either achieve full or negligible migration definitely show migration to be a source of hysteresis [104]; while clear evidence of the role of flow history in the migration effects is found, we have not succeeded in reliably measuring the concentration field. The TC flow of suspensions has developed broader interest, and mention should also be made of very recent work. Dash *et al.* [105] extended consideration of suspension TC flow to $Re(\phi) = O(1000)$ and $\phi \leqslant 0.4$, applying torque measurement along with frequency analysis of the observed flow structures; Ramesh and Alam [106] have recently explored a taller device, i.e., with axial length L yielding a larger L/δ than prior work, and report additional novel flow states.

After just a few years of intensive study, the behavior of suspensions in TC flow is seen to be so rich that the range of behavior verges on bewildering. At the largest concentrations explored, $\phi = 0.3$ in Majji *et al.* [102] and up to $\phi = 0.4$ in Dash *et al.*, the role of shear-induced migration in an inertial flow must be considered. There is thus reason to expect significant advancement in knowledge of suspension fluid mechanics from exploration of TC flow, but there is a clear need for theoretically based modeling, in order to both organize our questions and systematize our understanding as it develops. Analysis by Majji *et al.* indicated that the SVF and RIB states exhibited by suspensions are the same as states found in pure fluids but under different flow conditions, namely when the two cylinders are counter-rotating; this suggests that consideration of the behavior described in this section as an alteration of the TC dynamical system by the addition of rigid particles is a fruitful direction. Examination of the suspension TC flow under conditions of both cylinders rotating is rather obviously expected to be enlightening.

2. Pipe-flow stability of suspensions

As suspensions of many types are pumped through piping networks in a vast range of applications, this and the next section consider pressure-driven flows. We begin with the straight circular pipe flow, which in addition to its relevance in practice also presents a difficult stability problem. The TC flow discussed in the prior section passes through a series of transitions before reaching turbulence, and for the pure fluid these are well established. In addition, the flow is amenable to linear stability analysis [107]. By contrast, the instability of Newtonian Poiseuille flow involves a direct transition from laminar to turbulent flow through a subcritical bifurcation: Pressure-driven pipe flow at any Re is linearly stable [108]. It is, however, one of the well-known facts taught in basic fluid mechanics that the transition to turbulence of straight pipe flow occurs reliably near $Re = \rho DU/\eta_0 = 2000$ if perturbations are sufficient.

Matas *et al.* [109] considered this transition for suspensions, with the goal of understanding how convected disturbances by the neutrally buoyant particles (these caused predominantly by the force dipoles, or stresslets) affect the behavior. This was done by strongly disturbing the flow at its entrance to a straight glass pipe, which resulted in transition as expected for critical $Re_c \approx 2100$. The determination of the critical Re_c was based on measurement of the power spectrum of fluctuations in the differential pressure across the experimental test section of the pipe: At the onset of intermittent turbulence, the spectrum shows a characteristic low-frequency peak absent in the laminar flow. While suspensions exhibit small-scale unsteadiness due to the constantly changing particle arrangement, the signal was distinctly different in the two regimes. Flows were studied in two pipes of different diameter D. The range of spherical particle size to pipe diameter was $10 \leqslant D/2a \leqslant 350$ with some dispersion for each particle size. The central result was that the larger particles, with $D/2a < 65$, induced an apparent onset of turbulence at $Re(\phi) = \rho DU/\eta(\phi) < 2100$, in fact as low

as $Re(\phi) \approx 800$ for $D/2a = 10 \pm 1$. Note that $Re(\phi)$ uses the apparent viscosity, but even using the lower pure fluid viscosity a substantial reduction in Re for onset of intermittent turbulence was seen. By contrast, for smaller particles ($D/2a > 65$), the onset remained at $Re_c(\phi) \approx 2100$ for $\phi < 0.25$, above which solid fraction the transition was actually delayed to larger Re. Small particles seem to be satisfactorily described for the pipe-flow transition by an effective viscosity up to moderate ϕ and then they add a damping that has not been explained; among other possibilities, this may be related to either their position in the pipe (migration effects) or to inertia at the microscale, both noted in prior sections.

The lower-Re onset of transition for larger particles appears to be related to the triggering of turbulence in the simple shear of a wall-bounded plane Couette flow (PCF) by wires or single spheres. The case with a spherical bead (rather than extended wire) held fixed on the midplane so that it exerts a force dipole (torque and stresslet) but no net force is closer to the case of suspended particles (which exert a stresslet but only small fluctuating torques, being free to rotate in the flow). The bead case was initially studied by Bottin *et al.* [110] with more details provided in a separate study [111]. These experimental studies considered finite-amplitude disturbances triggering instability of PCF, which is linearly stable at any Re [108] but found to be unstable to finite perturbations at $Re = \rho U h/\eta_0 \approx 750$ [112]; here U is the speed of either wall relative to zero at the midplane, and $2h$ is the distance between the parallel walls. The onsets of intermittent and full turbulence were found to be triggered as low as $Re = 280$ and 320, respectively, for a wire of diameter $d/2h \approx 0.06$, and thus with $Re_p = (d/2h)^2 Re \approx 1$. A more localized process of vortex growth away from a bead was described. Numerical work by Mikulencak and Morris [41] found that local vortex structures on a single sphere or cylinder appear only at much larger Re_p, implying the need to consider the interaction of the disturbance flow at the surface with the bulk shear flow to explain vortex growth at this Re_p; numerical study of this issue has not been presented to date.

Recent experimental study of the elevated-ϕ pipe flow has shed further light on this issue: The work of Hogendoorn and Poelma [113] suggests significant differences from the pure fluid in the near transition region, specifically that the so-called turbulent "puffs" do not appear. This appears to be consistent with the findings of Agrawal *et al.* [114] that describe three regimes for the transition, one like the pure fluid for $\phi < 0.05$, one a suspension mechanism at $\phi > 0.125$, and a mixed regime at ϕ between these values. The behavior may be geometry specific, as pipe flow exhibits traveling wave solutions [115] at $Re < 2000$ that may factor into the behavior. With this caveat, fully resolved multiparticle simulations have explored related issues, e.g., by application of the force coupling method to study the influence of neutrally buoyant particles on large scale structures in turbulent PCF [116]. Simulations by the immersed boundary [117] and lattice-Boltzmann [118] methods have been used to explore the behavior of turbulent particle-laden flows in pressure-driven channel flows. This demonstrated ability to examine the particle-resolved behavior above the transition, i.e., under conditions of low-Re turbulence, shows the promise of direct simulation as a means of exposing the mechanism of suspension pipe-flow instability at lower Reynolds number than the pure fluid.

VI. TOWARD GEOMETRICALLY COMPLEX FLOWS: BIFURCATING CONDUITS

Here the goal is to move toward more general, geometrically complex, flows of suspensions with significant inertia. The focus will be on flows in channels that undergo bifurcations, i.e., one inlet to two outlet branches, as this allows exploration of the impact of certain of the issues considered above, while also raising new questions. While we do not try to model details of either case directly, these are also flows that play significant roles in applications such as hydraulic fracturing [119] and blood flow [120].

Before considering the inertial cases, we note that some related flows studied for suspensions in the Stokes-flow regime involve issues noted above. Bifurcating channels have been considered experimentally using magnetic resonance imaging (MRI) techniques [121], focusing on particle migration and its effect on the flow split. Modeling of bifurcating channels using the diffusive flux approach [122] or closely related flow around obstacles by the SBM [95] reproduce a number of

the basic features, indicating that for Stokes flow our understanding of the coupling of rheology to the migration works satisfactorily for some confidence in its use in applications, at least for monodisperse suspensions.

In bifurcation flow of particle-laden fluids, relative particle concentration in the two branches is often of primary interest [123,124]. The bulk flow in an asymmetric T-channel, in which one branch at the bifurcation continues straight while the other makes a 90-deg turn, was examined in early work by Bugliarello and Hsiao [125]; this work imposed flow rates in the two branches to determine the solid fraction "flow splits" for understanding of hemodynamics (blood flow). This same topic was considered for different geometry by Doyeux *et al.* for deformable particles in a model of a bifurcating blood vessel. The goal in this work was to explore the basis for the Zweifach-Fung effect [126], in which an abundance of red blood cells, beyond expectations in terms of the mean concentration, is found to go to the higher flow rate branch. However, recent work revisiting suspension flows in the noted asymmetric T [127] and the symmetric form [128], where the outlets are both at 90 deg from the inlet, shows that these flows represent significant challenges to our ability to predict the observed behavior. In particular, for almost all ϕ, a simple effective viscosity estimate of the behavior yields poor agreement, and for some conditions outright conflict, with results of experiment. This necessitates two-phase computations that track the solid fraction and velocity fields to determine the flow splits (of bulk suspension and of particles) to the outlet branches in the asymmetric T with acceptable accuracy.

In a combination of experiments and two simulation methods—suspension lattice-Boltzmann (LB) [129] and immersed boundary (IB) [130]—we [127] examined the flow at equal pressure drop and channel length in each outlet branch in an asymmetric T-channel with square cross section. This work considered neutrally buoyant suspensions for particles with diameter yielding $2a/D = 0.1$ and 0.2, where D is the channel side length, for mean solid fractions of $\phi_0 \leqslant 0.3$. Accessible flow rates generated $Re \leqslant 900$ for the pure fluid, while lower $Re(\phi)$ were achieved for the suspensions with their elevated effective viscosities. For a pure fluid, the fraction of inlet flow rate to the straight branch (continuation of the inlet) increases with Re, because it is more difficult to deflect the fluid into the side branch as its inertia increases. This trend is reduced as ϕ increases, and rather strikingly, for $\phi \geqslant 0.20$ the fraction of the total flow to the side branch was larger over the entire range of flow rates studied [the maximum $Re(\phi) \approx 320$ and 200 for $\phi = 0.20$ and 0.30, respectively]. The tendency of more material to exit through the side branch is explainable based on shear-induced migration at the higher ϕ in the inlet branch of $L/D = 58$, such that the particle-depleted layer at the walls is pulled more easily into the side channel, a phenomenon previously described in blood flow where a cell-free layer appears due to the Fahreus-Lindqvist effect [120], and the material continuing in the straight branch has increased ϕ ($\phi_\parallel > \phi_0$) relative to the side branch ($\phi_\perp < \phi_0$). This slows the flow in the outlet branch as the mean pressure gradient across each outlet branch is the same. Thus, the solid fraction variation induced by the upstream channel flow affects the hydraulic, i.e., the flow rate vs pressure drop, relationship in the outlet channel. To illustrate these points, concentration profiles computed in the study [127] are reproduced in Fig. 3, with (a) showing the fully developed (i.e., for $L/D \to \infty$) ϕ determined by LB simulation illustrated at $Re(\phi) = 50$, showing a transition from inertially dominated migration to the peripheries to a combination of inertial and shear-induced migration (with more accumulation at the center of the cross section) as solid fraction increases from $\phi = 0.05$ to 0.15 and 0.25. Figure 3(b) shows the IB computations of particle locations at $L/D = 58$, corresponding to the cross section of the inlet channel at the entry corner of the side branch, for $\phi = 0.05$ at $Re = 50$ and 300. These figures color code the particles and the streamline regions with respect to their outlet channel, showing that as Re increases, the gray zone of streamlines shrinks and detaches from the entire periphery, with flow to the side branch drawn from the entire viscous layer near the boundary. The complex partitioning of particles and fluid into the two branches as a function of ϕ and Re, as well as the side channel dimension [131], requires consideration of the coupled effects of migration and the streamline split of the two-phase flow. As inertial migration interacting with SIM seen here as well as in pipe flow [67] presents an unresolved modeling challenge, there appears to be a significant gap in our ability to predict these flows.

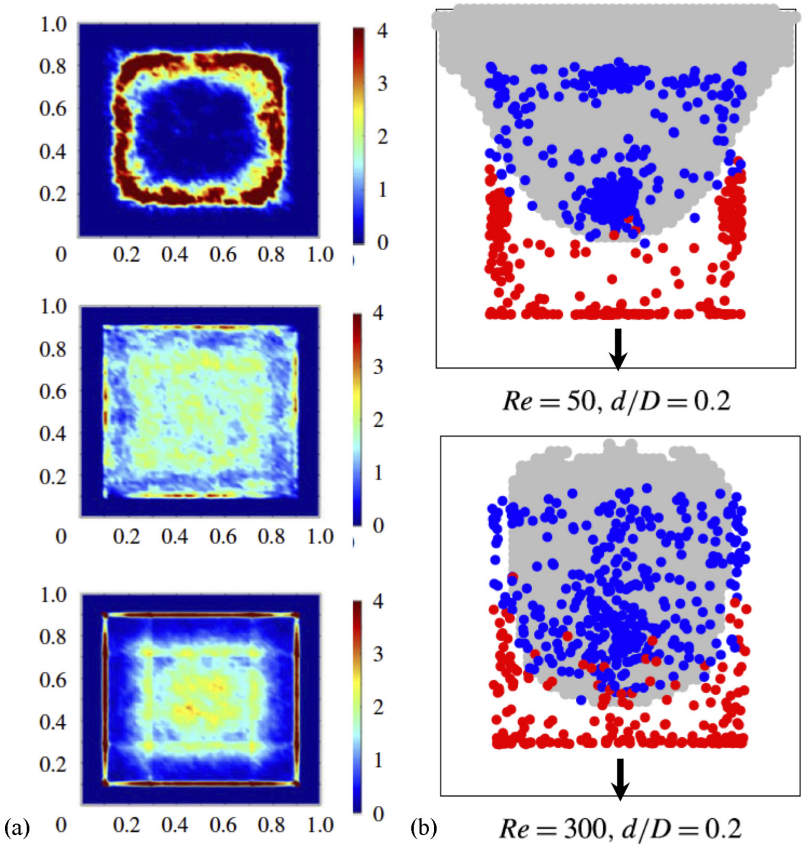

FIG. 3. Simulated migration in an asymmetric T for $d/D = 0.2$. (a) Lattice-Boltzmann suspension simulations in a straight square channel for fully developed migration ($L/D \to \infty$) at $Re = 46$ and (from top to bottom) $\phi = 0.05, 0.15$, and 0.25. Color bar indicates relative solid fraction and differs between the three cases. (b) Immersed boundary method calculations at $\phi = 0.05$ and $Re = 50$ and $Re = 300$ at the cross section of the leading corner of the side channel in the asymmetric T geometry equivalent to the experimental geometry (at $L/D = 58$). The arrows point in the direction of the side channel; blue and red particles continue in the straight channel or are diverted to the side channel, respectively, largely but not completely following the gray and white zones of streamlines which continue straight and divert to the side channel, respectively. Note that at $Re = 300$, the side channel draws flow from the entire periphery of the cross section.

Figure 4 shows that both flow structure and the overall features of the solid distribution are well captured by the IB method computations, which is of special value because the solid fraction is difficult to probe experimentally. This figure also indicates the importance of the boundary condition in suspension flows, as the inability of the particle centers to reach the near-wall streamlines implies that the particles are rarely found in the recirculating regions associated with the two separation regions. These recirculations are not fully closed owing to complex three-dimensional flows; simplification of the flow to two dimensions (i.e., a slit channel with side draw) would therefore be misleading owing to this behavior, as well as to the noted flow from the cross-section periphery to the side channel, illustrated by Fig. 3(b).

The interaction of particles with the boundary in a symmetric T-channel involves a different issue, as there is strong wall-normal flow carrying the particles into the stagnation zone at the bifurcation. Such a flow is relevant to suspension flow past an obstacle, or due to impeller mixing of particle-laden liquids, as well as to various microfluidic applications. In the symmetric T with

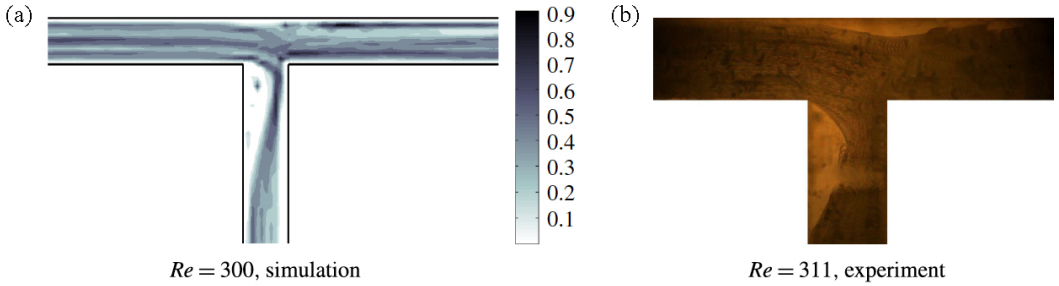

FIG. 4. Comparison of simulation and experiment for $\phi = 0.2$: (a) immersed-boundary method simulations at $Re(\phi) = 300$ and (b) experiment at $Re(\phi) = 311$, for particles of size $2a/D = 0.2$ with a the particle radius, and D the channel side length.

square cross section, with equal pressure drops in the outlet branches, the flow exhibits a set of counter-rotating vortices in each outlet channel for $Re = O(100)$ as described by [132] in work in a microfluidic environment; this work considered the dynamics of dilute particles denser than the fluid, with some approaching neutral buoyancy, and described conditions necessary for their impact with the wall, while a later study [133] developed a coupled analytical and numerical approach to deduce the trapping regions associated with the vortex regions in T and V-shaped channels, for particles lighter than the fluid. These studies raise the questions of neutrally buoyant particle dynamics in normal motion toward, and potential impact on, a wall. Particle motion in the wall-normal Hiemenz-Homann [134,135] flow at a stagnation point has been considered [136,137] and this work shows that for a particle of $a/\delta_{\mathrm{HH}} > 2$ impact can be expected for physically reasonable levels of surface asperities; here $\delta_{\mathrm{HH}} = \sqrt{\nu/B}$ is the Hiemenz-Homann boundary layer scaling, with B the strain rate in the stagnation zone and ν the kinematic viscosity. A further observation (alluded to above in mention of outright conflicts with experiment of an apparent viscosity estimate of behavior) is that, in the symmetric T-channel [128], even when the bulk $Re(\phi)$ is matched to the pure fluid value of $Re = 200$ by increase of the flow rate in proportion to the apparent shear viscosity, vortices seen at $\phi = 0$ and 0.10 are damped for $\phi = 0.20$ and completely suppressed for $\phi = 0.30$. Note that separations from the corners entering the two outlet channels are largely unchanged by the increase of volume fraction. This flow thus exhibits pronounced two-phase influence, and suggests strongly that the wall-normal flow of a suspension at elevated inertia dissipates energy at levels far above the expectation based on effective viscosity modeling: The conjecture is that the rapid deceleration at the wall causes intense squeezing flows in the films between the nearest particles and wall, and between the next-farther layer of particles and this one, and so forth, that lead to this added dissipation.

VII. PERSPECTIVE

From foundations in microhydrodynamics formulated into constitutive descriptions, we have a physically well-understood material model in the near-hard-sphere suspension. When restricted to neutral buoyancy, this material remains homogeneous and allows us to probe the behaviors uniquely resulting from fluid-particle and particle-particle interactions. The 50 years since the landmark work of Batchelor [1] have witnessed a remarkable increase in understanding of the range of behaviors in suspensions. We now have firm understanding of their non-Newtonian rheology and its coupling to bulk flow phenomena in Stokes flow, while particle migration associated with inertia is routinely harnessed for application and we can now ask its effects on flow stability.

Yet for prediction of the bulk material behavior, the goal of a continuum description—i.e., a true fluid mechanics of suspensions—is in its infancy. To elaborate on this point, consider the previous section, which delved into suspension flow under conditions where various phenomena

described in earlier sections occur together, in a T geometry. While this is clearly not the approach to elucidate individual phenomena, it appears that this is one necessary direction of study toward the predictive ability needed for broad utility of the large body of understanding that has been developed on suspensions.

The leading perspective that is offered here is that research in fluid mechanics of suspensions must now synthesize understanding of various topics into predictive models, develop computational algorithms designed specifically for their solution and thus targeted to the two-phase behavior, and confront the predictions with experimental characterization of the behavior; this offers challenges that are theoretical, computational, and experimental. Finding the appropriate problems to address the various points requires careful thought and some creativity: To merge with our developed understanding of single-phase fluid mechanics, revisiting classic problems, in the spirit of the examinations of Taylor-Couette flow described in Sec. V B, may be appropriate, but there may be a need for new paradigm problems.

At a more specific level, three basic directions that require attention come to mind based on my own experience. One is the full characterization of the general rheology in arbitrary flows of suspensions: Relative to Newtonian fluids, this is a pervasive problem in non-Newtonian materials, and is particularly important in suspensions because of the tendency of particles to migrate under the influence of the rheology. This will require novel experiments and simulations, to determine the bulk properties and explain them based on microhydrodynamics. A second direction, related to the first, is to develop methods to account for the role of history in suspension flows. Because of migration of particles, the influence of the flow history is pronounced, and once again the prior section showing the influence of the upstream migration on flow at a bifurcation provides an example. Thus history can refer to spatial effects such as the axial flow in a conduit, or it may refer to time under flow as in the Taylor-Couette flow and the resulting hysteresis. Even when the particles are Brownian and have a relaxation mechanism, relaxation in suspension flows is typically slow. Thus the influence of earlier flow will persist after flow cessation and may be seen at restart or in a flow reversal [54]. However, a more striking effect of the history is in changing the macroscopic state of the material by inducing concentration gradients. This impacts strongly on the material properties and thus the timescales within the material; as an example, consider the migration to a central core in pressure-driven flow, and the question of how this divides at a bifurcation. The third direction of inquiry is boundary interactions and boundary conditions. When considering inertial migration, the distance from the boundary is critical, and this implies that description of this migration mechanism is not constitutive, i.e., knowledge of only the local conditions about a particle does not allow prediction of inertial migration. The boundary conditions in both normal and tangential motion at solid boundaries affect the behavior of the particle phase in quite significant ways, as discussed in Sec. VI, and have received relatively little attention. Finally, the mention of boundaries is a convenient place to point out that this article has left aside the issues associated with suspensions in free-surface flows. This class of flows plays a role in consideration of rheometry of suspensions, as the particles may protrude at the free boundary and the capillary stress affects normal stress measurements [35,138] and may play a role in the instability known as edge fracture [139], while numerous applications such as drop formation relevant in combustion of slurry fuels or coating are impacted by suspensions at free surfaces.

The motivations for a fluid mechanics of suspensions are many. As the fundamental questions in suspensions range over scales from contact mechanics to bulk flows, the opportunities for inquiry are abundant and given their value in practice, advances will be welcomed in many fields of application.

ACKNOWLEDGMENTS

This work was prepared to capture the message of the Stanley Corrsin Award lecture presented at the 2019 APS DFD meeting in Seattle. While the award citation specifically notes microstructure, the implications of the microstructure for bulk flow behavior have provided the motivation for much of the author's body of work, so the lecture adopted the theme of development of a fluid

mechanics of suspensions. The preparation of this manuscript was supported in part by NSF Award 1916879 and in part by the FERMat Federation through "NEMESIS—From the Nanoscale to Eulerian Modeling: Engineering and Science In Suspensions" a Chaire d'Attractivité provided by IDEX Université de Toulouse. The work described was made possible through talented students and post-doctoral researchers, and benefited from numerous collaborations, among which those with John Brady (Caltech), Élisabeth Guazzelli (CNRS), and Morton Denn (City College of New York) have been especially influential.

[1] G. K. Batchelor, The stress system in a suspension of force-free particles, J. Fluid Mech. **41**, 545 (1970).
[2] H. A. Barnes, A review of the rheology of filled viscoelastic systems, in *Rheology Reviews* (British Society of Rheology, 2003).
[3] G. D'Avino and P. L. Maffettone, Particle dynamics in viscoelastic liquids, J. Non-Newtonian Fluid Mech. **215**, 80 (2015).
[4] J. F. Brady and J. F. Morris, Microstructure of strongly sheared suspensions and its impact on rheology and diffusion, J. Fluid Mech. **348**, 103 (1997).
[5] J. F. Brady and G. Bossis, Stokesian dynamics, Annu. Rev. Fluid Mech. **20**, 111 (1988).
[6] E. Guazzelli and J. F. Morris, *A Physical Introduction to Suspension Dynamics* (Cambridge University Press, Cambridge, 2012).
[7] R. C. Ball and J. R. Melrose, Lubrication breakdown in hydrodynamic simulations of concentrated colloids, Adv. Colloid Interface Sci. **59**, 19 (1995).
[8] J. R. Melrose and R. C. Ball, The pathological behaviour of sheared hard spheres with hydrodynamic interactions, Europhys. Lett. **32**, 535 (1995).
[9] G. A. Barabino, M. O. Platt, and D. K. Kaul, Sickle cell biomechanics, Annu. Rev. Biomed. Eng. **12**, 345 (2010).
[10] E. J. Hinch, A perspective of Batchelor's research in micro-hydrodynamics, J. Fluid Mech. **663**, 8 (2010).
[11] A. Einstein, Eine neue bestimmun der molekuldimensionen, Ann. Phys. **19**, 289 (1906).
[12] J. Happel and H. Brenner, *Low Reynolds Number Hydrodynamics: With Special Applications to Particulate Media*, Springer Science & Business Media (Springer, New York, 2012).
[13] G. K. Batchelor and J. T. Green, The hydrodynamic interaction of two small freely-moving spheres in a linear flow field, J. Fluid Mech. **56**, 375 (1972).
[14] G. K. Batchelor and J. T. Green, The determination of the bulk stress in a suspension of spherical particles to order c^2, J. Fluid Mech. **56**, 401 (1972).
[15] G. K. Batchelor, Sedimentation in a dilute dispersion of spheres, J. Fluid Mech. **52**, 245 (1972).
[16] D. J. Jeffrey and Y. Onishi, Calculation of the resistance and mobility functions for two unequal rigid spheres in low-Reynolds-number flow, J. Fluid Mech. **139**, 261 (1984).
[17] D. J. Jeffrey, The calculation of the low Reynolds number resistance functions for two unequal spheres, Phys. Fluids A **4**, 16 (1992).
[18] A. Sierou and J. F. Brady, Accelerated Stokesian dynamics simulations, J. Fluid Mech. **448**, 115 (2001).
[19] A. M Fiore and J. W. Swan, Fast Stokesian dynamics, J. Fluid Mech. **878**, 544 (2019).
[20] J. F. Morris, Shear thickening of concentrated suspensions: Recent developments and relation to other phenomena, Annu. Rev. Fluid Mech. **52**, 121 (2020).
[21] J. Mewis and N. J. Wagner, *Colloidal Suspension Rheology* (Cambridge University Press, Cambridge, 2011).
[22] T. N. Phung, J. F. Brady, and G. Bossis, Stokesian Dynamics simulation of Brownian suspensions, J. Fluid Mech. **313**, 181 (1996).
[23] D. R. Foss and J. F. Brady, Structure, diffusion and rheology of Brownian suspensions by Stokesian dynamics simulation, J. Fluid Mech. **407**, 167 (2000).
[24] J. C. van der Werff and C. G. De Kruif, Hard-sphere colloidal dispersions: The scaling of rheological properties with particle size, volume fraction, and shear rate, J. Rheol. **33**, 421 (1989).

[25] P. D'Haene, J. Mewis, and G. G. Fuller, Scattering dichroism measurements of flow-induced structure of a shear thickening suspension, J. Colloid Interface Sci. **156**, 350 (1993).
[26] J. F. Morris and B. Katyal, Microstructure from simulated Brownian suspension flows at large shear rate, Phys. Fluids **14**, 1920 (2002).
[27] I. E. Zarraga, D. A. Hill, and D. T. Leighton, The characterization of the total stress of concentrated suspensions of noncolloidal spheres in Newtonian fluids, J. Rheol. **44**, 185 (2000).
[28] C. Gamonpilas, J. F. Morris, and M. M. Denn, Shear and normal stress measurements in non-Brownian monodisperse and bidisperse suspensions, J. Rheol. **60**, 289 (2016).
[29] C. D. Cwalina and N. J. Wagner, Material properties of the shear-thickened state in concentrated near hard-sphere colloidal dispersions, J. Rheol. **58**, 949 (2014).
[30] J. R. Royer, D. L. Blair, and S. D. Hudson, Rheological Signature of Frictional Interactions in Shear Thickening Suspensions, Phys. Rev. Lett. **116**, 188301 (2016).
[31] I. E. Zarraga, D. A. Hill, and D. T. Leighton, Normal stresses and free surface deformation in concentrated suspensions of noncolloidal spheres in a viscoelastic fluid, J. Rheol. **45**, 1065 (2001).
[32] A. Zrehen and A. Ramachandran, Demonstration of Secondary Currents in the Pressure-Driven Flow of a Concentrated Suspension Through a Square Conduit, Phys. Rev. Lett. **110**, 018306 (2013).
[33] J. F. Morris and F. Boulay, Curvilinear flows of noncolloidal suspensions: The role of normal stresses, J. Rheol. **43**, 1213 (1999).
[34] A. Deboeuf, G. Gauthier, J. Martin, Y. Yurkovetsky, and J. F. Morris, Particle Pressure in a Sheared Suspension: A Bridge from Osmosis to Granular Dilatancy, Phys. Rev. Lett. **102**, 108301 (2009).
[35] S. Garland, G. Gauthier, J. Martin, and J. F. Morris, Normal stress measurements in sheared non-Brownian suspensions, J. Rheol. **57**, 71 (2013).
[36] F. Boyer, E. Guazzelli, and O. Pouliquen, Unifying Suspension and Granular Rheology, Phys. Rev. Lett. **107**, 188301 (2011).
[37] D. Prasad and H. K. Kytömaa, Particle stress and viscous compaction during shear of dense suspensions, Int. J. Multiphase Flow **21**, 775 (1995).
[38] C. J. Lin, J. H. Peery, and W. R. Schowalter, Simple shear flow round a rigid sphere: Inertial effects and suspension rheology, J. Fluid Mech. **44**, 1 (1970).
[39] X. Li and K. Sarkar, Effects of inertia on the rheology of a dilute emulsion of drops in shear, J. Rheol. **49**, 1377 (2005).
[40] N. A. Patankar and H. H. Hu, Finite Reynolds number effect on the rheology of a dilute suspension of neutrally buoyant circular particles in a Newtonian fluid, Int. J. Multiphase Flow **28**, 409 (2002).
[41] D. R. Mikulencak and J. F. Morris, Stationary shear flow around fixed and free bodies at finite Reynolds number, J. Fluid Mech. **520**, 215 (2004).
[42] P. M. Kulkarni and J. F. Morris, Pair-sphere trajectories in finite Reynolds number shear flow, J. Fluid Mech. **596**, 413 (2008).
[43] H. Haddadi and J. F. Morris, Topology of pair-sphere trajectories in finite inertia suspension shear flow and its effects on microstructure and rheology, Phys. Fluids **27**, 043302 (2015).
[44] J. F. Brady and M. Vicic, Normal stresses in colloidal dispersions, J. Rheol. **39**, 545 (1995).
[45] G. K. Batchelor, The effect of Brownian motion on the bulk stress in a suspension of spherical particles, J. Fluid Mech. **83**, 97 (1977).
[46] H. J. Wilson, An analytic form for the pair distribution function and rheology of a dilute suspension of rough spheres in plane strain flow, J. Fluid Mech. **534**, 97 (2005).
[47] F. Parsi and F. Gadala-Maria, Fore-and-aft asymmetry in a concentrated suspension of solid spheres, J. Rheol. **31**, 725 (1987).
[48] D. J. Jeffrey, J. F. Morris, and J. F. Brady, The pressure moments for two rigid spheres in low-Reynolds-number flow, Phys. Fluids A **5**, 2317 (1993).
[49] Y. Yurkovetsky and J. F. Morris, Particle pressure in sheared Brownian suspensions, J. Rheol. **52**, 141 (2008).
[50] J. J. Stickel and R. L. Powell, Fluid mechanics and rheology of dense suspensions, Annu. Rev. Fluid Mech. **37**, 129 (2005).

[51] J. F. Morris, A review of microstructure in concentrated suspensions and its implications for rheology and bulk flow, Rheol. Acta **48**, 909 (2009).
[52] E. Nazockdast and J. F. Morris, Microstructural theory and the rheology of concentrated colloidal suspensions, J. Fluid Mech. **713**, 420 (2012).
[53] A. Scacchi, M. Krüger, and J. M. Brader, Driven colloidal fluids: Construction of dynamical density functional theories from exactly solvable limits, J. Phys.: Condens. Matter **28**, 244023 (2016).
[54] R. N. Chacko, R. Mari, S. M. Fielding, and E. Cates, M, Shear reversal in dense suspensions: The challenge to fabric evolution models from simulation data, J. Fluid Mech. **847**, 700 (2018).
[55] J. J. J. Gillissen and H. J. Wilson, Modeling sphere suspension microstructure and stress, Phys. Rev. E **98**, 033119 (2018).
[56] O. Ozenda, P. Saramito, and G. Chambon, A new rate-independent tensorial model for suspensions of noncolloidal rigid particles in Newtonian fluids, J. Rheol. **62**, 889 (2018).
[57] R. Seto, R. Mari, J. F. Morris, and M. M. Denn, Discontinuous Shear Thickening of Frictional Hard-Sphere Suspensions, Phys. Rev. Lett. **111**, 218301 (2013).
[58] M. Wyart and M. E. Cates, Discontinuous Shear Thickening without Inertia in Dense Non-Brownian Suspensions, Phys. Rev. Lett. **112**, 098302 (2014).
[59] R. Mari, R. Seto, J. F. Morris, and M. M. Denn, Shear thickening, frictionless and frictional rheologies in non-Brownian suspensions, J. Rheol. **58**, 1693 (2014).
[60] M. Wang, S. Jamali, and J. F. Brady, A hydrodynamic model for discontinuous shear-thickening in dense suspensions, J. Rheol. **64**, 379 (2020).
[61] E. Del Gado and J. F. Morris, Preface: Physics of dense suspensions, J. Rheol. **64**, 223 (2020).
[62] B. Saint-Michel, T. Gibaud, and S. Manneville, Uncovering Instabilities in the Spatiotemporal Dynamics of a Shear-Thickening Cornstarch Suspension, Phys. Rev. X **8**, 031006 (2018).
[63] R. N. Chacko, R. Mari, M. E. Cates, and S. M. Fielding, Dynamic Vorticity Banding in Discontinuously Shear Thickening Suspensions, Phys. Rev. Lett. **121**, 108003 (2018).
[64] R. J. Larsen, J.-W. Kim, C. F. Zukoski, and D. A. Weitz, Fluctuations in flow produced by competition between apparent wall slip and dilatancy, Rheol. Acta **53**, 333 (2014).
[65] M. J. MacDonald and S. J. Muller, Experimental study of shear-induced migration of polymers in dilute solutions, J. Rheol. **40**, 259 (1996).
[66] J. R. Brown, E. O. Fridjonsson, J. D. Seymour, and S. L. Codd, Nuclear magnetic resonance measurement of shear-induced particle migration in Brownian suspensions, Phys. Fluids **21**, 093301 (2009).
[67] M. Han, C. Kim, M. Kim, and S. Lee, Particle migration in tube flow of suspension, J. Rheol. **43**, 1157 (1999).
[68] G. Segré and A. Silberberg, Radial particle displacements in Poiseuille flow of suspensions, Nature **189**, 209 (1961).
[69] P. G. Saffman, The lift on small sphere in a slow shear flow, J. Fluid Mech. **22**, 385 (1965).
[70] B. P. Ho and L. G. Leal, Inertial migration of rigid spheres in two-dimensional unidirectional flow, J. Fluid Mech. **65**, 365 (1974).
[71] J. A. Schonberg and E. Hinch, Inertial migration of a sphere in Poiseuille flow, J. Fluid Mech. **203**, 517 (1989).
[72] E. S. Asmolov, The inertial lift on a spherical particle in a plane Poiseuille flow at a large channel Reynolds number, J. Fluid Mech. **381**, 63 (1999).
[73] J. P. Matas, J. F. Morris, and E. Guazzelli, Lateral force on a rigid sphere in large-inertia laminar pipe flow, J. Fluid Mech. **621**, 59 (2009).
[74] J. P. Matas, J. F. Morris, and E. Guazzelli, Inertial migration of rigid spherical particles in Poiseuille flow, J. Fluid Mech. **515**, 171 (2004).
[75] Y. Morita, T. Itano, and M. Sugihara-Seki, Equilibrium radial positions of neutrally buoyant spherical particles over the circular cross-section in Poiseuille flow, J. Fluid Mech. **813**, 750 (2017).
[76] J. S. Halow and G. B. Wills, Experimental observations of sphere migration in Couette systems, Ind. Eng. Chem. Fund. **9**, 603 (1970).
[77] M. V. Majji and J. F. Morris, Inertial migration of particles in Taylor-Couette flows, Phys. Fluids **30**, 033303 (2018).

[78] A. A. S. Bhagat, S. S. Kuntaegowdanahalli, and I. Papautsky, Enhanced particle filtration in straight microchannels using shear-modulated inertial migration, Phys. Fluids **20**, 1 (2008).
[79] B. Chun and A. C. J. Ladd, Inertial migration of neutrally buoyant particles in a square duct: An investigation of multiple equilibrium positions, Phys. Fluids **18**, 1 (2006).
[80] D. D. Carlo, D. Irimia, R. G. Tompkins, and M. Toner, Continuous inertial focusing, ordering, and separation of particles in microchannels, Proc. Natl. Acad. Sci. USA **104**, 18892 (2007).
[81] S. Kahkeshani, H. Haddadi, and D. Di Carlo, Preferred interparticle spacings in trains of particles in inertial microchannel flows, J. Fluid Mech. **786**, R3 (2016).
[82] J. P. Matas, V. Glezer, E. Guazzelli, and J. F. Morris, Trains of particles in finite-Reynolds-number pipe flow, Phys. Fluids **16**, 4192 (2004).
[83] G. Segré and A. Silberberg, Behaviour of macroscopic rigid spheres in Poiseuille flow Part 2. Experimental results and interpretation, J. Fluid Mech. **14**, 136 (1962).
[84] J. M. Martel and M. Toner, Particle focusing in curved microfluidic channels, Sci. Rep. **3**, 3340 (2013).
[85] J. M. Martel and M. Toner, Inertial focusing in microfluidics, Ann. Rev. Biomed. Eng. **16**, 371 (2014).
[86] D. T. Leighton and A. Acrivos, The shear-induced migration of particles in concentrated suspensions, J. Fluid Mech. **181**, 415 (1987).
[87] A. Karnis, H. L. Goldsmith, and S. G. Mason, The kinetics of flowing dispersions: I. Concentrated suspensions of rigid particles, J. Colloid Interface Sci. **22**, 531 (1966).
[88] C. J. Koh, P. Hookham, and L. G. Leal, An experimental investigation of concentrated suspension flows in a rectangular channel, J. Fluid Mech. **266**, 1 (1994).
[89] P. R. Nott and J. F. Brady, Pressure-driven flow of suspensions: Simulation and theory, J. Fluid Mech. **275**, 157 (1994).
[90] R. J. Phillips, R. C. Armstrong, R. A. Brown, A. L. Graham, and J. R. Abbott, A constitutive equation for concentrated suspensions that accounts for shear-induced particle migration, Phys. Fluids. A **4**, 30 (1992).
[91] J. F. Richardson and W. N. Zaki, The sedimentation of a suspension of uniform spheres under conditions of viscous flow, Chem. Eng. Sci. **3**, 65 (1954).
[92] R. H. Davis and A. Acrivos, Sedimentation of noncolloidal particles at low Reynolds numbers, Annu. Rev. Fluid Mech. **17**, 91 (1985).
[93] M. Frank, D. Anderson, E. R. Weeks, and J. F. Morris, Particle migration in pressure-driven flow of a Brownian suspension, J. Fluid Mech. **493**, 363 (2003).
[94] K. von Pfeil, M. D. Graham, D. J. Klingenberg, and J. F. Morris, Pattern Formation in Flowing Electrorheological Fluids, Phys. Rev. Lett. **88**, 188301 (2002).
[95] R. M. Miller, J. P. Singh, and J. F. Morris, Suspension flow modeling for general geometries, Chem. Eng. Sci. **64**, 4597 (2009).
[96] D. Merhi, E. Lemaire, G. Bossis, and F. Moukalled, Particle migration in a concentrated suspension flowing between rotating parallel plates: Investigation of diffusion flux coefficients, J. Rheol. **49**, 1429 (2005).
[97] H. Giesekus, Sekundarstromungen in viskoelastischen flussigkeiten bei stationarer und periodischer bewegung, Rheol. Acta **4**, 85 (1965).
[98] A. Ramachandran and D. T. Leighton, The influence of secondary flows induced by normal stress differences on the shear-induced migration of particles in concentrated suspensions, J. Fluid Mech. **603**, 207 (2008).
[99] D. Dherbecourt, S. Charton, F. Lamadie, S. Cazin, and E. Climent, Experimental study of enhanced mixing induced by particles in Taylor–Couette flows, Chem. Eng. Res. Design **108**, 109 (2016).
[100] C. D. Andereck, S. S. Liu, and H. L. Swinney, Flow regimes in a circular Couette system with independently rotating cylinders, J. Fluid Mech. **164**, 155 (1986).
[101] M. E. Ali, D. Mitra, J. A. Schwille, and R. M. Lueptow, Hydrodynamic stability of a suspension in cylindrical Couette flow, Phys. Fluids **14**, 1236 (2002).
[102] M. V. Majji, S. Banerjee, and J. F. Morris, Inertial flow transitions of a suspension in Taylor-Couette geometry, J. Fluid Mech. **835**, 936 (2018).

[103] P. Ramesh, S. Bharadwaj, and M. Alam, Suspension Taylor–Couette flow: Co-existence of stationary and travelling waves, and the characteristics of Taylor vortices and spirals, J. Fluid Mech. **870**, 901 (2019).
[104] L. Baroudi, M. V. Majji, and J. F. Morris, Effect of inertial migration of particles on flow transitions of a suspension Taylor-Couette flow, Phys. Rev. Fluids (to be published).
[105] A. Dash, A. Anantharaman, and C. Poelma, Particle-laden Taylor-Couette flows: Higher order transitions and evidence for azimuthally localized wavy vortices, J. Fluid Mech. **903**, A20 (2020).
[106] P. Ramesh and M. Alam, Interpenetrating spiral vortices and other coexisting states in suspension Taylor-Couette flow, Phys. Rev. Fluids **5**, 042301 (2020).
[107] S. Chandrasekhar, The stability of viscous flow between rotating cylinders, Proc. R. Soc. London Ser. A **246**, 301 (1958).
[108] P. G. Drazin and W. H. Reid, *Hydrodynamic Stability* (Cambridge University Press, New York, 1985).
[109] J. P. Matas, J. F. Morris, and E. Guazzelli, Transition to Turbulence in Particulate Pipe Flow, Phys. Rev. Lett. **90**, 014501 (2003).
[110] S. Bottin, O. Dauchot, and F. Daviaud, Intermittency in a Locally Forced Plane Couette Flow, Phys. Rev. Lett. **79**, 4377 (1997).
[111] G. Antar, S. Bottin, O. Dauchot, F. Daviaud, and P. Manneville, Details on the intermittent transition to turbulence of a locally forced plane Couette flow, Exp. Fluids **34**, 324 (2003).
[112] H. Reichert, Uber die geschwindigkeitverteilung in einer geradlinigen turbulenten Couettesstromung, Z. Angew. Math. Mech. **36**, 26 (1956).
[113] W. Hogendoorn and C. Poelma, Particle-Laden Pipe Flows at High Volume Fractions Show Transition without Puffs, Phys. Rev. Lett. **121**, 194501 (2018).
[114] N. Agrawal, G. H. Choueiri, and B. Hof, Transition to Turbulence in Particle Laden Flows, Phys. Rev. Lett. **122**, 114502 (2019).
[115] B. Eckhardt, T. M. Schneider, B. Hof, and J. Westerweel, Turbulence transition in pipe flow, Annu. Rev. Fluid Mech. **39**, 447 (2007).
[116] G. Wang, M. Abbas, and E. Climent, Modulation of large-scale structures by neutrally buoyant and inertial finite-size particles in turbulent Couette flow, Phys. Rev. Fluids **2**, 084302 (2017).
[117] F. Picano, W. P. Breugem, and L. Brandt, Turbulent channel flow of dense suspensions of neutrally buoyant spheres, J. Fluid Mech. **764**, 463 (2015).
[118] L. P. Wang, C. Peng, Z. Guo, and Z. Yu, Lattice Boltzmann simulation of particle-laden turbulent channel flow, Comput. Fluids **124**, 226 (2016).
[119] A. A. Osiptsov, Fluid mechanics of hydraulic fracturing: A review, J. Pet. Sci. Eng. **156**, 513 (2017).
[120] T. J. Pedley, *The Fluid Mechanics of Large Blood Vessels* (Cambridge University Press, Cambridge, 2008).
[121] C. Xi and N. C. Shapley, Flow of a concentrated suspension through an axisymmetric bifurcation, J. Rheol. **52**, 625 (2008).
[122] S. Yadav, M. M. Reddy, and A. Singh, Shear-induced particle migration in three-dimensional bifurcation channel, Int. J. Multiphase Flow **76**, 1 (2015).
[123] Z. Y. Yan, A. Acrivos, and S. Weinbaum, Fluid skimming and particle entrainment into a small circular side pore, J. Fluid Mech. **229**, 1 (1991).
[124] B. W. Roberts and W. L. Olbricht, Flow-induced particulate separations, AIChE J. **49**, 2842 (2006).
[125] G. Bugliarello and G. C. C. Hsiao, Phase separation in suspensions flowing through bifurcations: A simplified hemodynamic model, Science **143**, 469 (1964).
[126] V. Doyeux, T. Podgorski, S. Peponas, M. Ismail, and G. Coupier, Spheres in the vicinity of a bifurcation: elucidating the Zweifach-Fung effect, J. Fluid Mech. **674**, 359 (2011).
[127] S. Manoorkar, S. Krishnan, O. Sedes, E. S. G. Shaqfeh, G. Iaccarino, and J. F. Morris, Suspension flow through an asymmetric T-junction, J. Fluid Mech. **844**, 247 (2018).
[128] S. Manoorkar and J. F. Morris, Particle motion in pressure-driven suspension flow through a symmetric T-channel, Int. J. Multiphase Flow **134**, 103447 (2020).
[129] A. J. C. Ladd, Numerical simulations of particulate suspensions via a discretized Boltzmann equation. Part 1. Theoretical foundation, J. Fluid Mech. **21**, 285 (1994).
[130] R. Mittal and G. Iaccarino, Immersed boundary methods, Annu. Rev. Fluid Mech. **37**, 239 (2005).

[131] S. Manoorkar, O. Sedes, and J. F. Morris, Particle transport in laboratory models of bifurcating fractures, J. Nat. Gas Sci. Eng. **33**, 1169 (2016).
[132] D. Vigolo, S. Raadl, and H. A. Stone, Unexpected trapping of particles at a T junction, Proc. Natl. Acad. Sci. USA **111**, 4770 (2014).
[133] D. Oettinger, J. T. Ault, H. A. Stone, and G. Haller, Invisible Anchors Trap Particles in Branching Junctions, Phys. Rev. Lett. **121**, 054502 (2018).
[134] K. Hiemenz, The boundary layer on a straight circular cylinder immersed in the uniform liquid flow, Dingler's Polytech. J. **326**, 321 (1911).
[135] F. Homann, Der Einfluss grosser Zähigkeit bei der Strömung um den Zylinder und um die Kugel, Z. Angew. Math. Mech. **16**, 153 (1936).
[136] Q. Li, M. Abbas, J. F. Morris, E. Climent, and J. Magnaudet, Near-wall dynamics of a neutrally buoyant spherical particle in an axisymmetric stagnation point flow, J. Fluid Mech. **892**, A32 (2020).
[137] Q. Li, M. Abbas, and J. F. Morris, Particle approach to a stagnation point at a wall: Viscous damping and collision dynamics, Phys. Rev. Fluids **5**, 104301 (2020).
[138] E. Brown and H. M. Jaeger, The role of dilation and confining stresses in shear thickening of dense suspensions, J. Rheol. **56**, 875 (2012).
[139] R. I. Tanner and S. Dai, Edge fracture in non-colloidal suspensions, J. Non-Newtonian Fluid Mech. **272**, 104171 (2019).